

Supplementary Figures and Tables

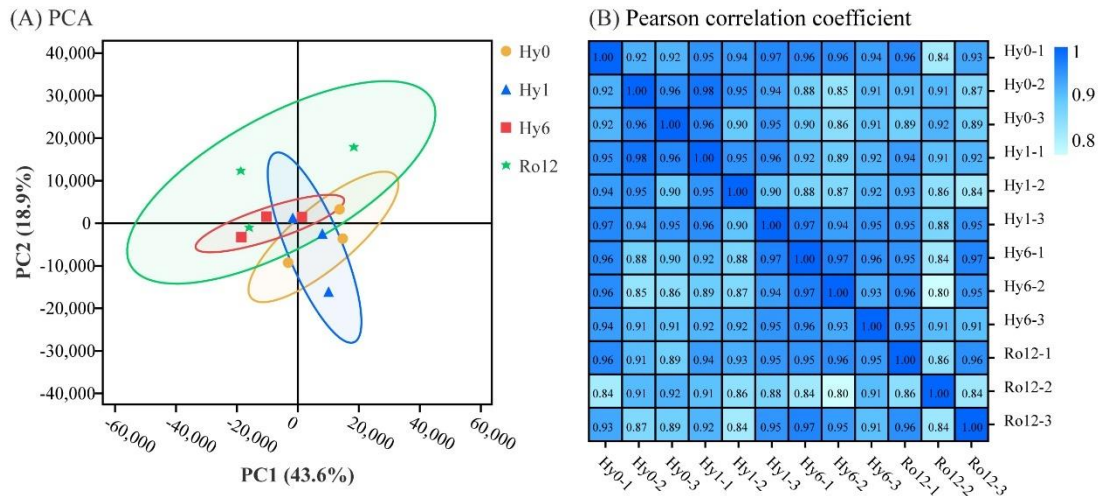


Figure S1. (A) Principal components analysis (PCA) and (B) Pearson's correlation coefficient between samples.

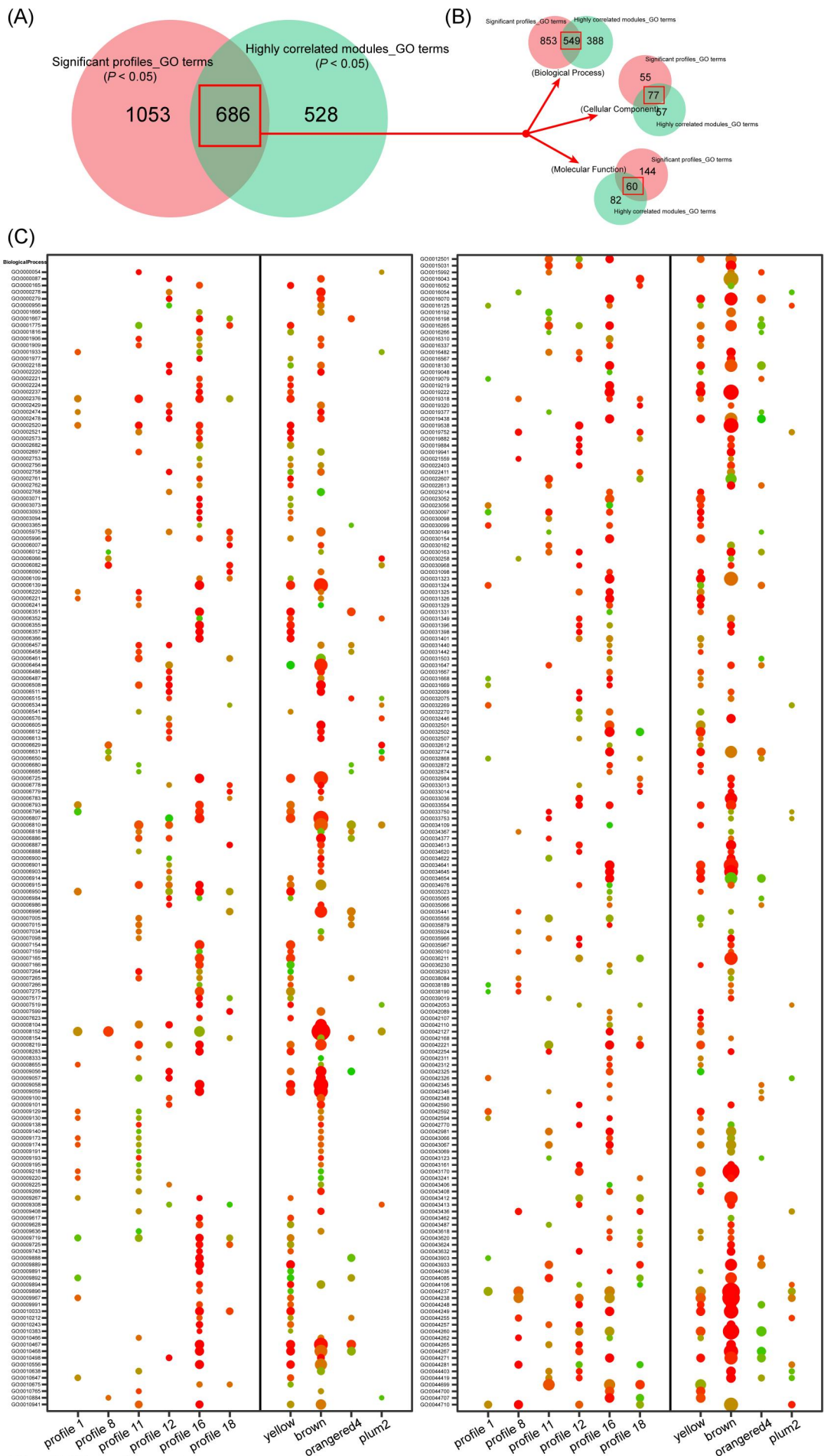


Fig. S2(See lenged on next page.)

(See Fig. S2 on previous page.)

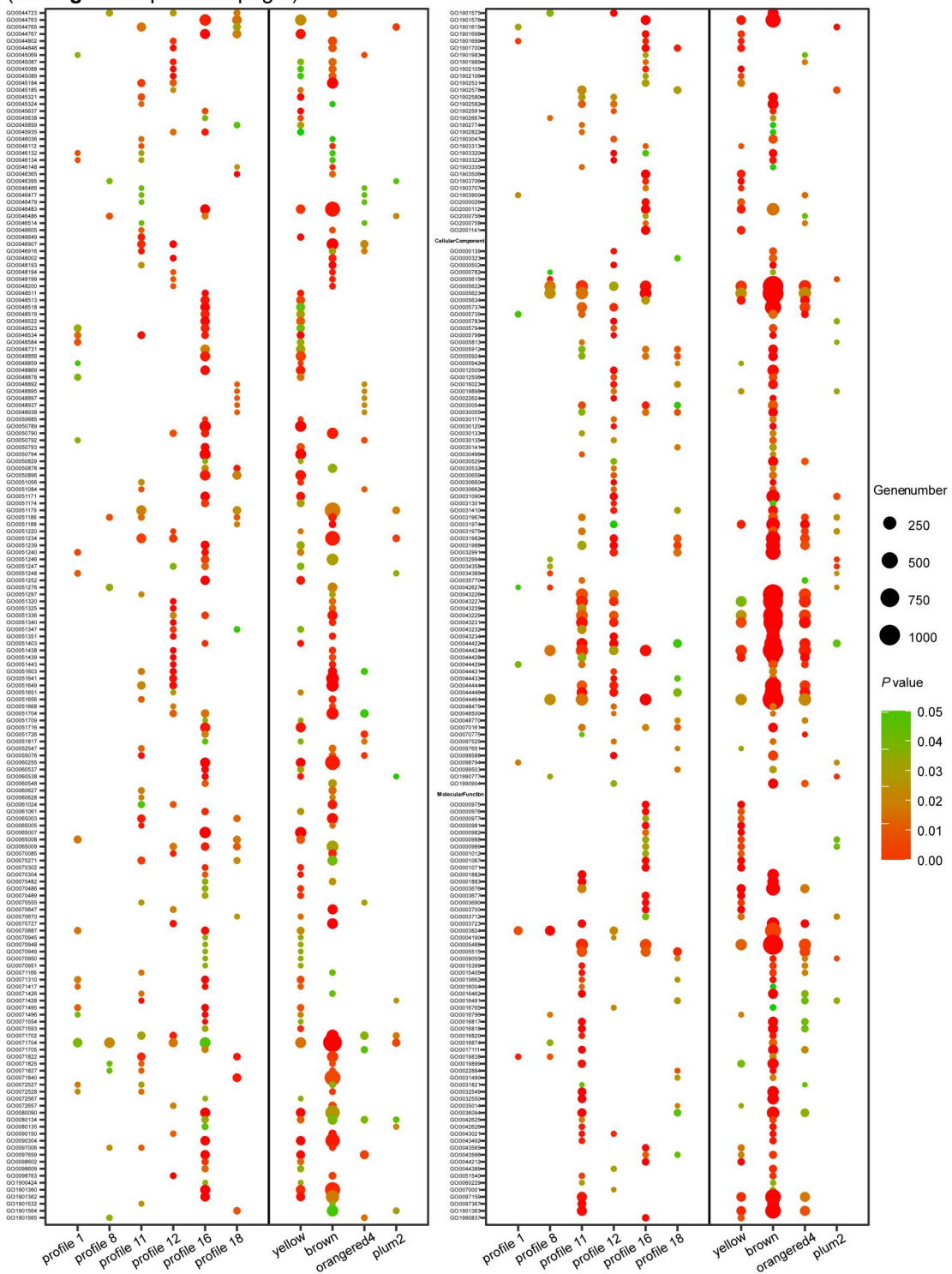
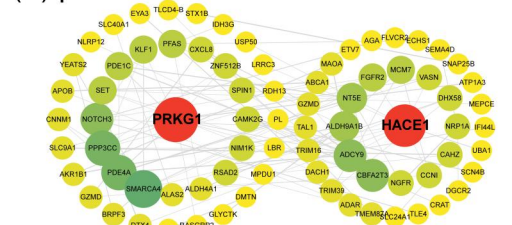
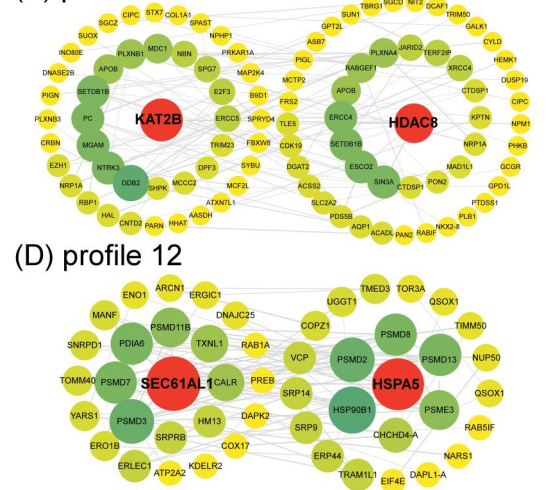


Figure S2. GO enrichment analysis. (A) Venn diagram of significant GO terms ($P < 0.05$) between six significant gene expression profiles (red circles) and four highly correlated modules (green circles). (B) Venn diagrams of significant GO term classifications. (C) The 686 common GO terms of significant profiles and highly correlated modules.

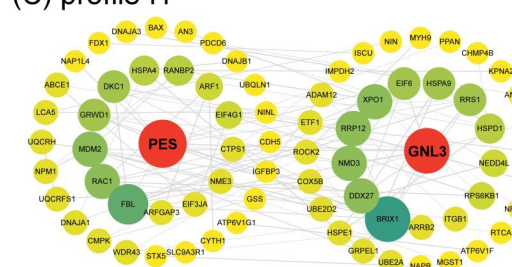
(A) profile 1



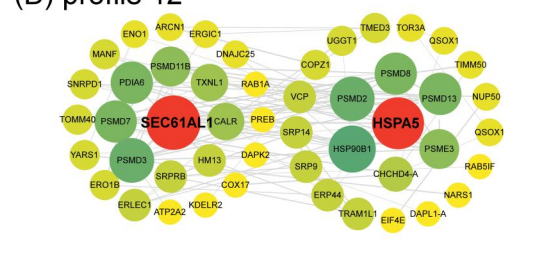
(B) profile 8



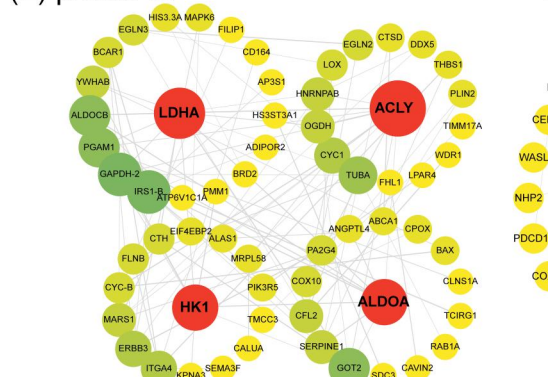
(C) profile 11



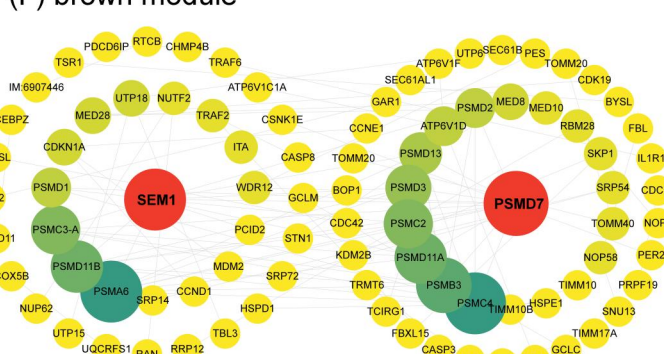
(D) profile 12



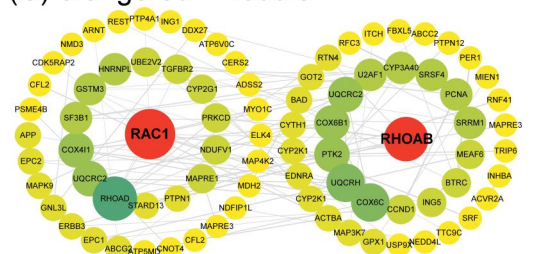
(E) profile 18



(F) brown module



(G) orangered4 module



(H) plum2 module

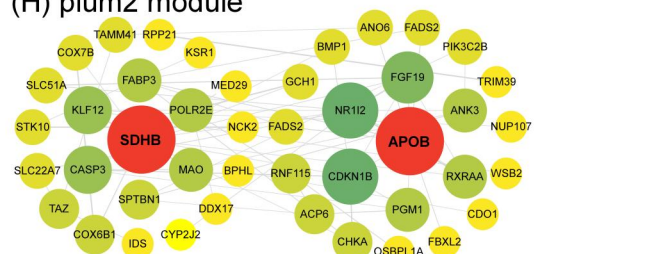


Figure S3. Protein-protein interaction (PPI) network analysis. The visualization of the first 100 interactions of profile 1 (A), profile 8 (B), profile 11 (C), profile 12 (D), profile 18 (E), brown module (F), orangered4 module (G), and plum2 module (H). The nodes represent genes; nodes size and color are related to the degree attribute of the PPI network; and larger size and deeper color indicate higher connectivity between genes. The edges indicate the connectivity between genes, the size of the edges is correlated with the combined score attribute, with a larger size representing a higher combined score.

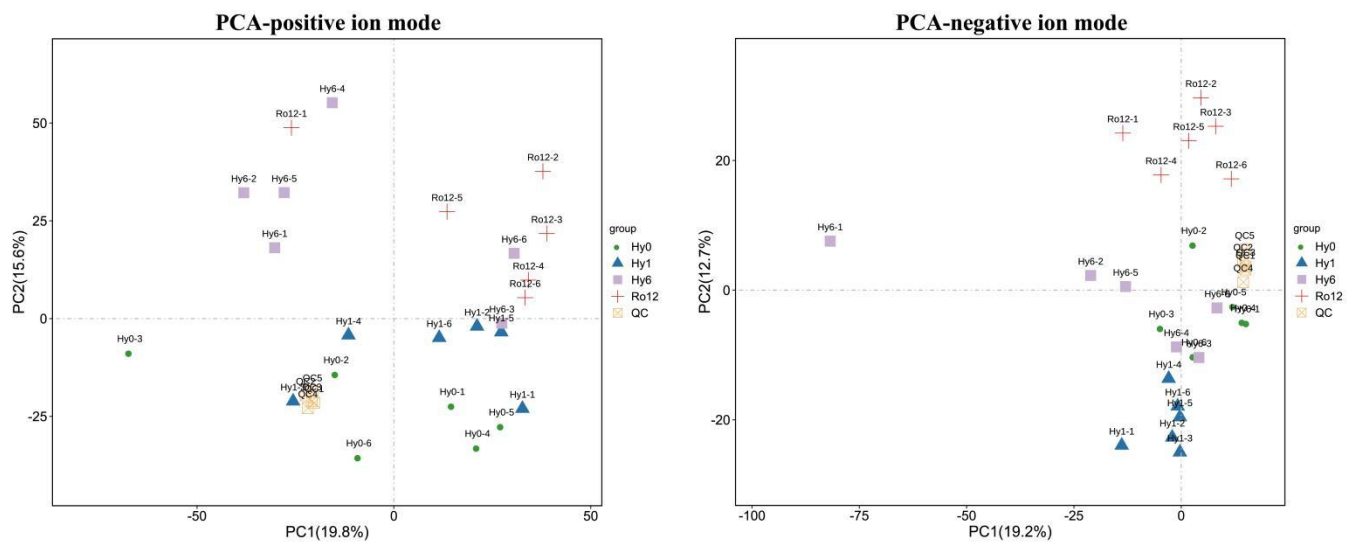


Figure S4. PCA analysis between treatment groups and QC sample under positive and negative ion modes.

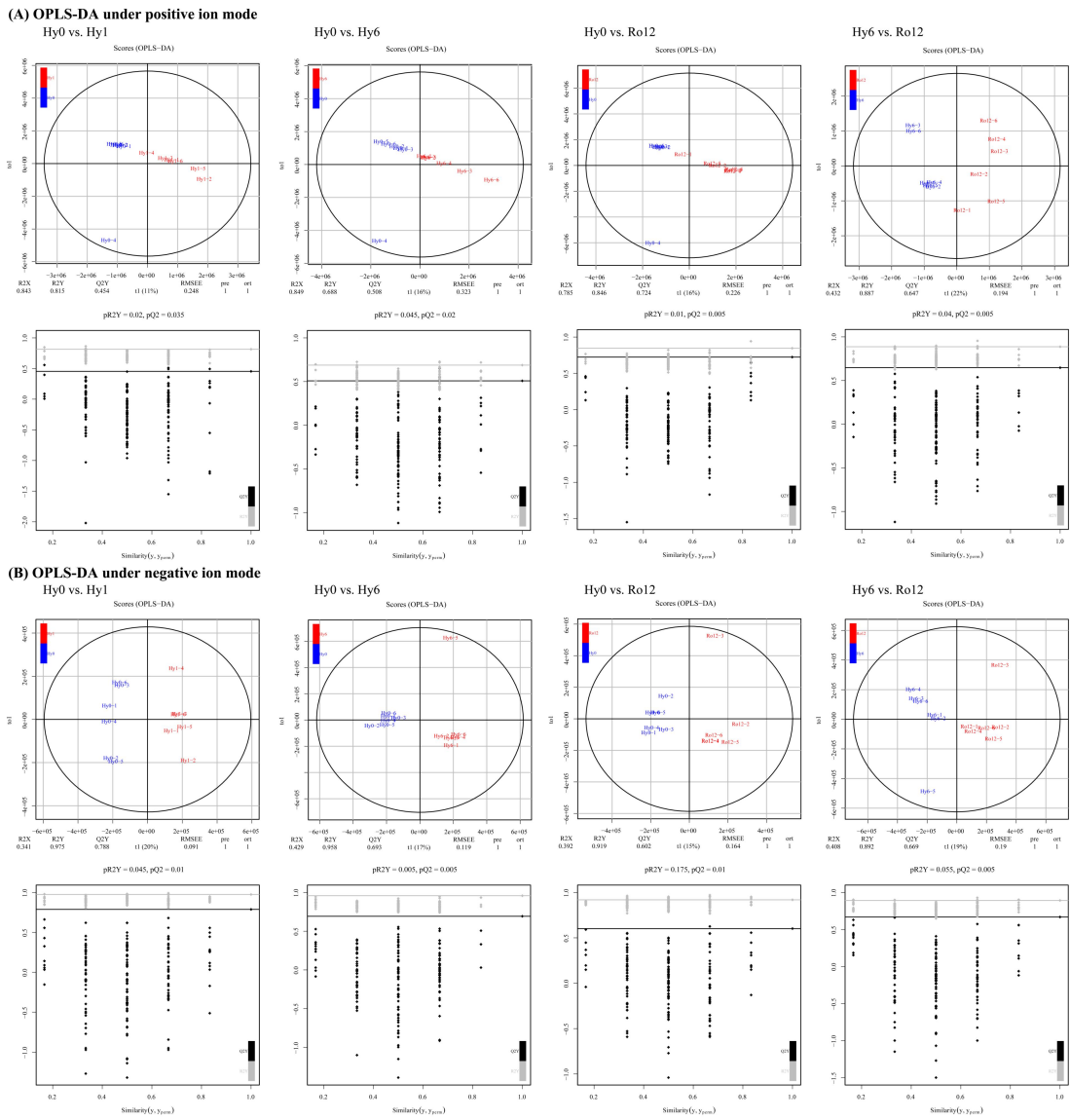


Figure S5. Orthogonal projection to latent structure-discriminant analysis (OPLS-DA) and permutation test under positive (A) and negative (B) ion modes.

Table S1 Specific gene number of 18 weighted gene co-expression network analysis (WGCNA) modules.

Module	Gene number	Module	Gene number	Module	Gene number
brown	2,215	darkturquoise	432	darkorange	153
lightsteelblue1	1,999	darkorange2	418	violet	137
brown4	1,315	darkmagenta	366	bisque4	93
black	615	darkred	356	plum2	89
lightpink4	502	yellow	344	thistle1	81
orangered4	433	green	335	grey	5

Table S2 Identification of metabolites under positive and negative ion modes.

Mode	Total	MS1	MS2	Known (MS1+ MS2)	Unknown
Positive ion mode	4,114	721	368	1,089	3,025
Negative ion mode	1,811	419	104	523	1,288

Table S3 The parameters of orthogonal partial least squares-discriminant analysis (OPLS-DA) model in Hy0 vs. Hy1, Hy0 vs. Hy6, Hy0 vs. Ro12, and Hy6 vs. Ro12 groups.

Mode	Group	R ² X	R ² Y	Q ² Y
Positive ion mode	Hy0 vs. Hy1	0.843	0.815	0.454
	Hy0 vs. Hy6	0.849	0.688	0.508
	Hy0 vs. Ro12	0.785	0.846	0.724
	Hy6 vs. Ro12	0.432	0.887	0.647
Negative ion mode	Hy0 vs. Hy1	0.341	0.975	0.788
	Hy0 vs. Hy6	0.429	0.958	0.693
	Hy0 vs. Ro12	0.392	0.919	0.602
	Hy6 vs. Ro12	0.408	0.892	0.669

Table S4 Specific primer sequences of ten randomly selected genes and one reference gene for qRT-PCR validation.

Condition	Parameters
UHPLC systems	
Column temperature	40°C
Chromatographic separation	Hypesil Gold column (C18)
Flow rate	17-min linear gradient with 0.2 mL·min ⁻¹
Positive ion mode: mobile phase A	0.1% formic acid in water
Positive ion mode: mobile phase B	Methanol
Negative ion mode: mobile phase A	5 mM ammonium bicarbonate in water (pH = 9.0)
Negative ion mode: mobile phase B	Methanol
Mass spectrometer	
Type	Electrospray ion source (ESI)
Electrospray voltage of positive ion mode (ESI+)	3.2 kV
Electrospray voltage of negative ion mode (ESI-)	2.5 kV
Ion source temperature	320°C
Sheath gas flow rate	40 arb
Aux gas flow rate	10 arb
Full scan	70,000 resolution
Scan range	80–1,000 m/z
Collision voltage	30 eV

Table S5 Specific primer sequences of ten randomly selected genes and one reference gene for qRT-PCR validation.

Gene_id	Gene_symbol	Forward primer (5'-3')	Reverse primer (5'-3')
/	β -actin*	CGTGCCTGACATCAAGGAGAA	AAGGAAGGAAGGCTGGAAGAGG
SCSFRI_TO_T_00039016.path1	<i>FOS</i>	GTCACCAGCGGGATCTTACTC	GAAATGGCTGTGACAGTGGG
SCSFRI_TO_T_00009724.path1	<i>BAX</i>	AGGGTGGTCGCACTGTTCTA	CAAGAAGACCCCCAACGTCT
SCSFRI_TO_T_00117137.path1	<i>MCL1</i>	ACCGATGTGTCGAGTTGCC	TTTCCAAAACGCCGTCCAC
SCSFRI_TO_T_00065768.path1	<i>CYC-B</i>	GGTCTGTTGGACGCAAGAC	CTTCTTTTGATGCCGGCGAA
SCSFRI_TO_T_00046973.path1	<i>HSP70</i>	ATACCTCGGCAACGTTAG	GTCCACCCAGATACTTCA
SCSFRI_TO_T_00135876.path1	<i>ALDOA</i>	AGAAGACGGATGACGGCAAG	GTCCAGACCTTGAGTGGTCG
SCSFRI_TO_T_00089332.path1	<i>LDHA</i>	CGTCAAGTACAGCCCCACT	TCTCCAATGATCCAGCCGTG
SCSFRI_TO_T_00015468.path1	<i>PCK1</i>	AACAACGGCCCTGTAACCC	TTGGCGATACGTGAGGCAAT
SCSFRI_TO_T_00000587.path1	<i>PNPLA2</i>	GCCAAGGTGCTGAGATGCT	GTGTCGGTACACCTCACAG
SCSFRI_TO_T_00095046.path1	<i>ACSL4</i>	GCGAGTTGGCAGTGGATTG	AGCAATAGCCTCTCCGA

*Reference: Chen et al., 2017.